(17) Nakashima, N.; Mataga, N. *Bull. Chem. Soc. Jpn.* **1973**, *46*, 3016.
(18) Cowley, D. J.; Healy, P. J. *Proc. R. Ir. Acad.* **1977**, 397.
(19) Rettig, W.; Wermuth, G.; Lippert, E. *Ber. Bunsen-Ges. Phys. Chem.* **1979**, *83*, 692.
(20) Tazuke, S.; Iwasaki, R. *Jpn.-US Polym. Symp. Prepr.* Kyoto, Japan **1985**, 199.
(21) Wermuth, G.; Rettig, W.; Lippert, E. *Ber. Bunsen-Ges. Phys. Chem.* **1981**, *85*, 64.
(22) Nishijima, Y.; Mito, Y. *Rep. Prog. Polym. Phys. Jpn.* **1967**, *10*, 139.
(23) de Gennes, P.-G. *Scaling Concepts in Polymer Physics*; Cornell Univ. Press: London, 1979; Chapter 3.
(24) Daoud, M.; Cotton, J. P.; Farnoux, B.; Jamink, G.; Benoit, H.; de Gennes, P.-G. *Macromolecules* **1975**, *8*, 804.
(25) In highly concentrated solutions, the Arrhenius plots had a break point at a certain temperature; the slope of the plot decreased suddenly below this point. T_b was determined at a cross point of two extended slopes from higher and lower temperature regions. The slope above T_b was slightly dependent on temperature, so that the different slopes gave different T_b. The temperature error bars in Figure 6 indicate this ambiguity of T_b.
(26) Williams, M. L.; Landel, R. F.; Ferry, J. D. *J. Am. Chem. Soc.* **1955**, *77*, 3701.
(27) Kelly, F. N.; Bueche, F. *J. Polym. Sci.* **1961**, *L*, 549.
(28) In the foregoing discussion, we accepted a priori the need of segment rotation to induce dual fluorescence. Baumann et al.[4b] criticized the simple TICT hypothesis proposed by Grabowski. Our present results, however, unequivocally show that a specific kind of chromophore motion is essential for the TICT phenomena.
(29) Hayashi, R.; Tazuke, S.; Frank, C. W. *Chem. Phys. Lett.*, in press.
(30) Al-Hassan, K. A.; Rettig, W. *Chem. Phys. Lett.* **1986**, *126*, 273.
(31) Hayashi, R.; Kitamura, N.; Tazuke, S. Abstract Book of Symposium on Photochemistry, Osaka, Japan, Nov. 1986.
(32) The ratio R and the rate to form the TICT state were increased when a longer excitation wavelength was used, whereas the temperature dependencies were not as affected by the excitation wavelength. This phenomenon and discussions will be reported in a forthcoming paper.

Dielectric Relaxation in Liquid Crystalline Poly(*p*-hydroxybenzoic acid-*co*-ethylene terephthalate)

Ulf W. Gedde,*† Douglas Buerger, and Richard H. Boyd

Department of Materials Science and Engineering and Department of Chemical Engineering, University of Utah, Salt Lake City, Utah 84112. *Received October 27, 1986*

ABSTRACT: Dielectric constant and loss have been measured over the frequency range 1 Hz–100 kHz from −180 to +180 °C for liquid crystalline poly(*p*-hydroxybenzoic acid-*co*-ethylene terephthalate) (P(HBA–ETP)) with molar ratios (HBA–ETP) of 0.6–0.4 and 0.8–0.2. In order of decreasing temperature, there are three transitions in these copolyesters: α_{HBA}, the glass–rubber transition of the HBA-rich phase, α_{ETP}, the glass–rubber transition of the ETP-rich phase, and β, a sub-glass transition that can be assigned to both the HBA-rich and ETP-rich phases. The symmetrically broadened β process shows a close resemblance to the β process in poly(ethylene terephthalate) (PETP) with regard to activation energy and width, but it occurs at progressively higher temperatures (isochronically) with increasing HBA content. The α_{ETP} occurs at lower temperatures than in PETP and has a width similar to that of semicrystalline PETP. The 0.6–0.4 copolymer exhibits a double α_{ETP}, which may indicate the presence of two different ETP-rich phases in this polymer.

Introduction

Polymers exhibiting liquid crystalline behavior in the melt, so-called thermotropic liquid crystalline polymers, have received considerable attention during the past decade. The mesomorphic melt phase is highly shear-sensitive and gives injection-molded solidified specimens with highly anisotropic mechanical properties. The modulus along the direction of orientation approaches the values of glass-fiber-reinforced thermoplastics. A distinct advantage of the thermotropic liquid crystalline polymers is their low melt viscosity when sheared, which makes them considerably easier to process than glass-fiber-reinforced thermoplastics.

The first example of a thermotropic polymer was reported in 1975 by Roviello et al.[1] and consisted of polyesters derived from aliphatic diacyl chlorides and *p,p'*-dihydroxy-α,α'-dimethylbenzalanine. A year later, Jackson and Kuhfuss[2] reported a thermotropic liquid crystalline copolyester based on *p*-hydroxybenzoic acid (HBA) and ethylene terephthalate (ETP). This polymer has served as a model compound, and numerous papers on this polymer can be found in the literature, e.g., ref 2–10.

Jackson and Kuhfuss[2] have presented NMR and WAXS data in support of a random distribution of the comonomer units in P(HBA–ETP) with molar composition 0.6–0.4. Nevertheless, the occurrence of two distinct and separate glass transitions in this polymer is clear evidence of the existence of separate phases rich in HBA and ETP.[4,5] Furthermore, electron microscopy and ESCA provide evidence of such a two-phase structure in the 0.6–0.4 copolymer.[6-8] The ETP-rich phase is discontinuous, exhibiting a domain size of the order of 1 μm. The molecular structure and morphology of P(HBA–ETP) with molar composition 0.8–0.2 is less disputed. Zachariades et al.[9,10] have shown that the distribution of the comonomer units is not random but that there are blocks of comonomers. These authors have also found some evidence for the existence of a minor amount of homopolymer of PHBA in the 0.8–0.2 copolymer samples. Transmission electron microscopy, electron diffraction, and X-ray analysis of the 0.8–0.2 copolymer indicate that long HBA sequences are present in discrete domains with a well-defined lamellar structure with a thickness of 200–400 Å.[9,10]

Dielectric studies of thermotropic liquid crystalline polymers have been relatively few.[11-16] Only one of these studies[16] deals with the polymer treated in the present paper. The authors report two dielectric relaxations in P(HBA–ETP) with molar composition 0.6–0.4: a β relaxation peaking at −30 °C (1 kHz) with an activation energy of 21 kJ mol^{-1} and an α relaxation centered at about 70 °C (1 kHz) with an activation energy of 500 kJ mol^{-1}. The authors claim that these data show a close resem-

† Present address: Department of Polymer Technology, The Royal Institute of Technology, S-100 44 Stockholm, Sweden.

0024-9297/87/2220-0988$01.50/0

blance with dielectric data for PETP homopolymer, although no conclusive evidence is presented for a phase assignment of the dielectric relaxations.

This paper presents data from dielectric measurements with a wider frequency range (1 Hz–100 kHz) than that utilized by Takase et al. (1 kHz–1 MHz). This is advantageous since the loss peaks are better resolved at lower frequencies. Furthermore, data for samples with two different compositions of comonomers and for the PHBA homopolymer are presented. These data are compared with the extensive data on PETP homopolymer by Coburn and Boyd,[17] making phase assignment possible for the dielectric relaxations.

Experimental Section

Dielectric Measurements. The dielectric apparatus consisted of a transformer arm ratio bridge (General Radio 1616 precision capacitance bridge), a microprocessor-controlled oscillator, and a two-phase detector (EG&G 5206 lock-in analyzer). The BCD output of the bridge was interfaced via three 16-bit ports on a parallel interface board to a laboratory computer (Charles River Data Systems LST 11/23 Base Model MF-211). The lock-in analyzer was connected to the CRDS Computer through a serial-line interface. The data logging from the bridge and the lock-in analyzer settings (frequency, sensitivity, phase angle, and time constant) were thus under the control of the CRDS and the microprocessors in the analyzer. Operator attention is confined to observation of the unbalanced signals on the detector and manual adjustment of the bridge balancing switches in response. The system is capable of satisfactory measurements from 1 Hz to 100 kHz.

The dielectric cell was of the parallel-plate design. In addition to the sample-occupied area another active area was provided for concurrent air or "empty cell" measurements. This was accomplished via four separate concentric rings in the lower plate. The innermost area was partially occupied by the sample. The gap between the inner area and the second ring creates a sample area guard. The third ring provided an air-filled active region whose distance from the upper plate was controlled by the sample thickness. The gaps between the second and third rings and between the third and fourth rings provide guards for the air-filled active electrode of the third ring. The empty cell capacitance was available at all temperatures simply by measuring the air-filled electrode capacitance.

The samples used were coated with gold–palladium in a vacuum sputterer. The diameter of the sample was always less than the diameter of the active center electrode. The capacitance corresponding to the empty area of the central electrode was subtracted from the measured inner electrode cell capacitance to obtain the actual sample capacitance.

The sample area was corrected for thermal expansion assuming expansional isotropy in relation to thermal expansion measurements.

Correction was also made for the sample surface roughness, which meant that the average sample thickness was smaller than the corresponding distance between the upper and lower electrodes. This correction was introduced as a scaling factor, typically reducing the values for the dielectric constant and loss by 10%.

The dielectric measurements were made isothermally at frequencies ranging from 1 Hz to 100 kHz preset in the driving program in the CRDS computer. A measurement at one frequency (12.3 kHz) served to determine the empty cell capacitance and sample thickness. The temperature was increased stepwise from low to high temperature for all specimens.

Two liquid crystalline copolyesters from Eastman Co., TN, poly(*p*-hydroxybenzoic acid (HBA)-*co*-ethylene terephthalate (ETP)) with molar composition 0.6–0.4 and 0.8–0.2, were studied. Information about the molecular structure and morphology can be found elsewhere.[2-10]

Samples were prepared by compression molding at 250 °C (P(HBA–ETP) 0.6–0.4) and 280 °C (P(HBA–ETP) 0.8–0.2) followed either by quenching in cold water or by slow cooling (1–2 °C/min) to room temperature. The two sets of samples are referred to respectively as "quenched" and "slow-cooled". The different samples were characterized with a Perkin-Elmer DSC-2 and the data from the thermal analysis are presented in Table I.

Table I
Thermal Analysis of Samples Studied

sample	$T_{g,low}$, °C	$T_{g,high}$, °C	$T_t/\Delta h$,[a] °C/(J/g)
0.6–0.4 slow cooled	61[b]	149	257/0.33
0.6–0.4 quenched	59[b]	161	255/0.21
0.8–0.2 slow cooled	71[c]	234	293/0.80
0.8–0.2 quenched	71[c]	232	298/0.42

[a] Endothermal first-order transition: peak temperature/heat of transition. [b] The change in specific heat associated with the glass transition amounts to 50 J(kmol ETP)$^{-1}$, which is the same as for fully amorphous PETP. [c] The change in specific heat amounts to about 70 ± 20 J(kmol ETP)$^{-1}$.

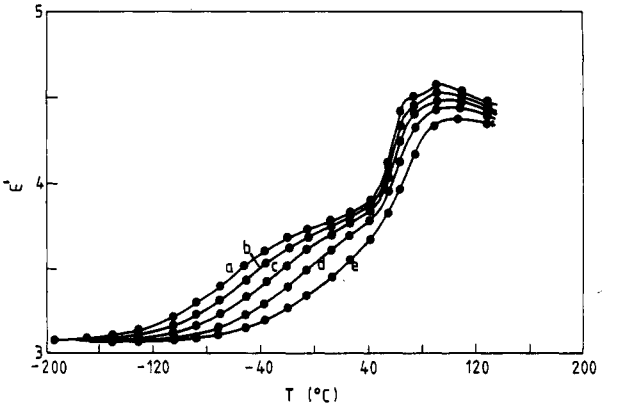

Figure 1. Dielectric constant (ϵ') of 0.6–0.4 P(HBA–ETP) (slow cooled) vs. temperature for the following frequencies: (a) 5 Hz; (b) 50 Hz; (c) 500 Hz; (d) 5000 Hz; (e) 50 000 Hz.

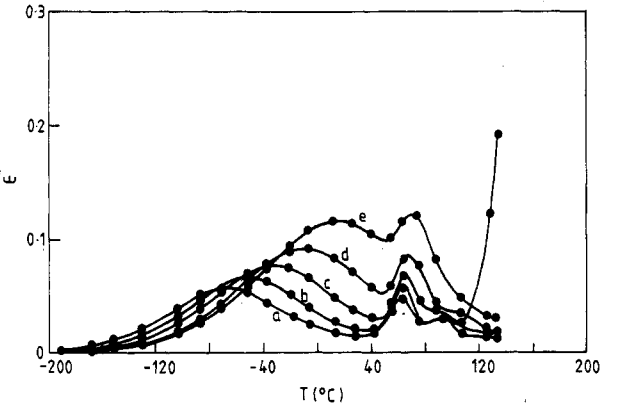

Figure 2. Dielectric loss (ϵ'') of 0.6–0.4 P(HBA–ETP) (slow cooled) vs. temperature at the following frequencies: (a) 5 Hz; (b) 50 Hz; (c) 500 Hz; (d) 5000 Hz; (e) 50 000 Hz.

A film-shaped sample containing homopolymer of PHBA (kindly supplied by Dr. Volksen, IBM Research, San Jose, CA) was prepared by dispersing PHBA in styrene, which at a later stage was polymerized by using benzoyl peroxide as initiator. The reaction was carried out under a nitrogen atmosphere. The choice of polystyrene as a matrix material was based on the fact that this polymer lacks dielectrically observable relaxations. This was verified by dielectric studies of the polystyrene prepared as described above.

Results and Discussion

Representative examples of the dielectric data for the copolyesters (dielectric constant and loss plotted vs. temperature) are shown in Figures 1–5. The data for the other samples exhibit a close resemblance to the curves presented and it can be concluded that the choice of thermal

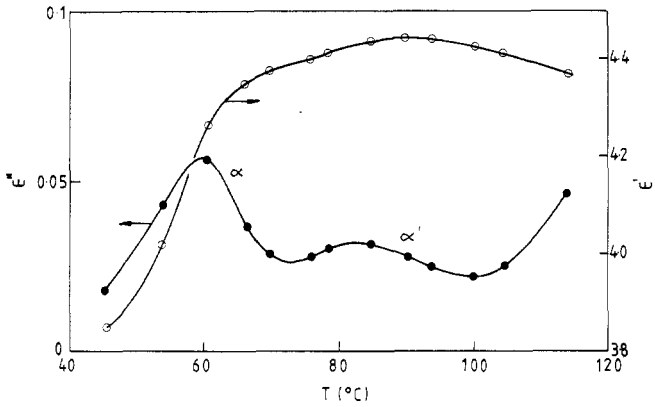

Figure 3. Dielectric loss (ϵ'') and dielectric constant (ϵ') of 0.6–0.4 P(HBA–ETP) (slow cooled) vs. temperature at 5 Hz.

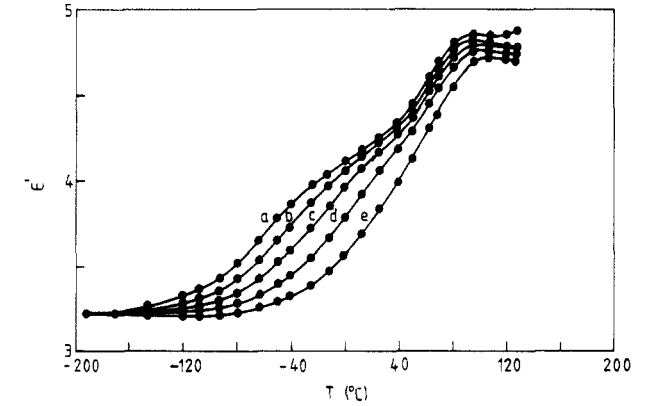

Figure 4. Dielectric constant (ϵ') of 0.8–0.2 P(HBA–ETP) (quenched) vs. temperature at the following frequencies: (a) 5 Hz; (b) 50 Hz; (c) 500 Hz; (d) 5000 Hz; (e) 50 000 Hz.

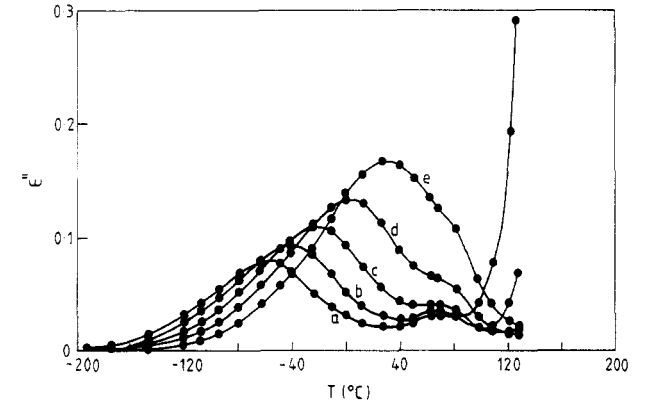

Figure 5. Dielectric loss (ϵ'') of 0.8–0.2 P(HBA–ETP) (quenched) vs. temperature at the following frequencies: (a) 5 Hz; (b) 50 Hz; (c) 500 Hz; (d) 5000 Hz; (e) 50 000 Hz.

pretreatment, slow cooling or quenching from temperatures above the upper glass transition, is not important for the dielectric behavior.

Three dielectric relaxations are observed in the 0.6–0.4 copolymer. They are denoted α', α, and β in order of decreasing temperature. The maximum in loss at 50 Hz occurs at +91 °C (α'), +64 °C (α), and −50 °C (β). Both α and β are known from the literature,[16] but the α' process is not reported in the paper by Takase et al.[16] It was not meaningful to make measurements revealing dielectric relaxations at temperatures above 120 °C due to the Maxwell–Wagner effect, which is indicated at high temperatures and low frequencies by a pronounced increase in ϵ' and ϵ'' with temperature. It is evident from DSC data that a high-temperature glass transition occurs in the

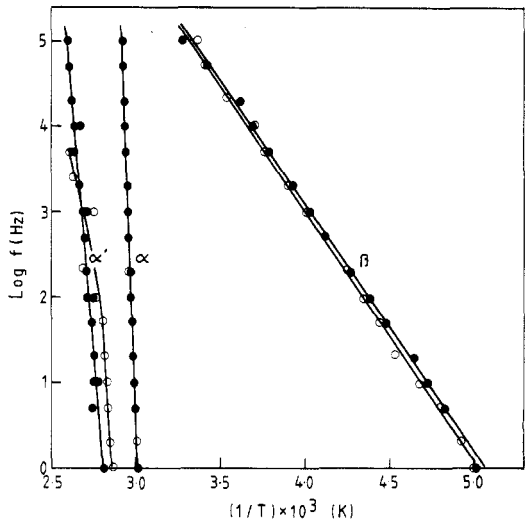

Figure 6. Temperature dependence of α', α, and β relaxations for the 0.6–0.4 P(HBA–ETP) samples: (●) slow cooled, (○) quenched. The data are obtained from isochronal ϵ''–T plots.

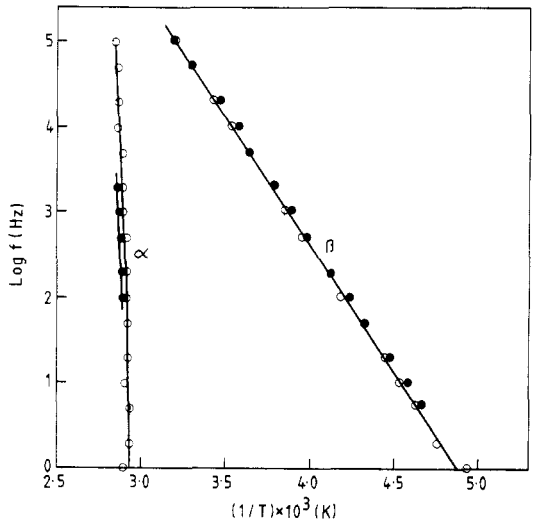

Figure 7. Temperature dependence of α and β relaxations for the 0.8–0.2 P(HBA–ETP) samples: (●) slowly cooled, (○) quenched. The data are obtained from isochronal ϵ''–T plots.

0.6–0.4 copolymer at about 150 °C (Table I).

Only two relaxations are distinguishable in the dielectric spectra of the 0.8–0.2 copolymer: α (70 °C) and β (−42 °C) at 50 Hz. A high-temperature glass transition is recorded at 230 °C by DSC (Table I). The high-temperature glass transition is not further discussed in this presentation.

β Process. The β process shows in terms of activation energy and temperature position a close resemblance to the sub-glass transition of PETP. The Arrhenius plots presented in Figures 6 and 7 show the similarity in behavior between the 0.6–0.4 and the 0.8–0.2 copolyesters. The activation energy is the same for both copolyesters and is insensitive to thermal history. A value of 56 kJ mol^{-1} is obtained for the copolyesters, which is very close indeed to the data for PETP of Coburn and Boyd.[17] The temperature-independent central relaxation time ($\tau_0°$, in the Arrhenius equation $\tau_0 = \tau_0° \exp(-\Delta E/RT)$) is slightly dependent on the composition: $\tau_0°(0.6\text{–}0.4) = 3\tau_0°$-(amorphous PETP) and $\tau_0°(0.8\text{–}0.2) = 10\tau_0°$(amorphous PETP). It should be pointed out that semicrystalline PETP has a $\tau_0°$ that is 1–3 times greater than that of fully amorphous PETP.[17]

The Argand plots, a typical example of which is presented in Figure 8, show that the β process is symmetrically

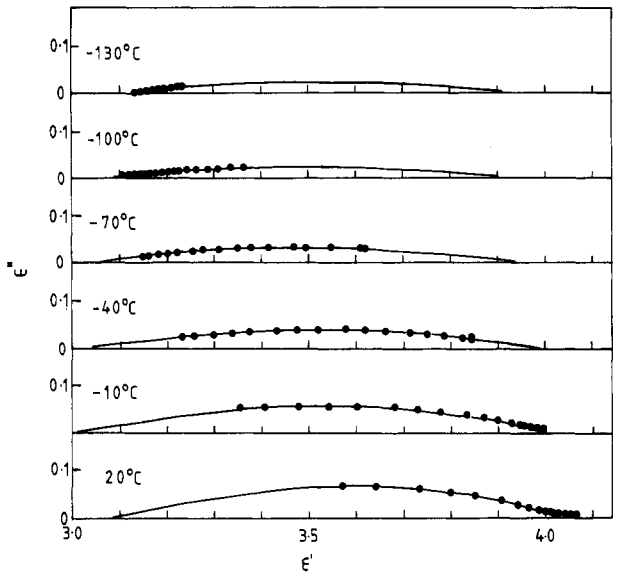

Figure 8. Argand diagrams (Cole–Cole plots) for 0.8–0.2 P(HBA–ETP) (slow cooled) in the temperature region of the β relaxation.

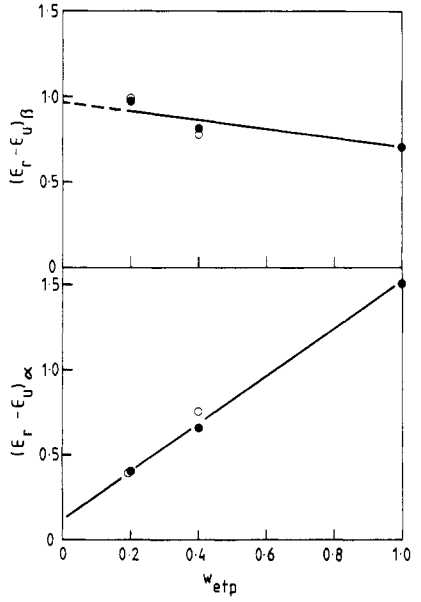

Figure 9. Relaxation strength ($\epsilon_R - \epsilon_U$) of $\alpha(\alpha + \alpha')$ ($\alpha''(\alpha + \alpha')$ in text) (at 90 °C) and β (at 20 °C) vs. the molar content of ETP. The relaxation strength data used for $w_{ETP} = 1$ are taken from Coburn and Boyd[17] and refer to quenched PETP with a crystallinity of 4%.

broadened and thus follows the Cole–Cole equation. It can therefore be described by four parameters: unrelaxed (ϵ_U) and relaxed (ϵ_R) dielectric constant, central relaxation time (τ_0), and symmetric broadening parameter ($\tilde{\alpha}$).

The relaxation strength ($\epsilon_R - \epsilon_U$) obtained from the intercepts of the circular arc in the Argand plot shows a striking independence of composition of the copolymer (Figure 9), which indicates that the β process should be assigned to both components of the copolymer, i.e., the ETP and HBA units.

The dielectric data of the homopolymer PHBA revealed no transition similar to the β process observed in the copolymer samples. It should be realized, however, that the PHBA sample is highly crystalline (80–90% according to ref 18) and thus not representative of the HBA component in the copolymers. It may be that the presence of the ETP comonomer is a prerequisite for the action of the HBA units in the β process. The temperature dependence of

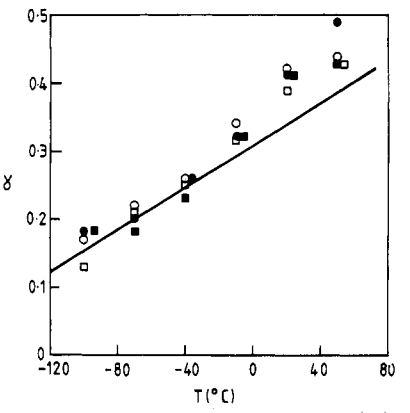

Figure 10. The symmetric width parameter ($\tilde{\alpha}$ in text) of the Havriliak–Negami equation vs. temperature for the β process. The solid line refers to quenched PETP (crystallinity = 4%) and is obtained from data by Coburn and Boyd.[17] (■, □) represents 0.6–0.4 P(HBA–ETP) quenched and slow cooled, respectively, and (●, ○) represents 0.8–0.2 P(HBA–ETP) quenched and slow cooled, respectively.

the width parameter presented in Figure 10 indicates the close resemblance between the copolyesters and PETP. It has been shown that the width parameter of the subglass transition (β) in PETP lacks morphological sensitivity.[17] It seems therefore reasonable that the contribution from the ETP-rich phase is not significantly affected by the presence of the constraining HBA-rich mesophase.

α Process. The relaxation strength of the $\alpha''(\alpha' + \alpha)$ process increases significantly with increasing content of ETP in the copolymer (Figure 9). In fact, the regression line has an intercept insignificantly separated from the origin in the plot shown in Figure 9, which is a clear argument for the assignment of the $\alpha''(\alpha' + \alpha)$ process to the ETP-rich phase.

In the 0.6–0.4 copolymer the glass–rubber transition is divided into two processes. This separation appears most clearly in the low-frequency data shown in Figure 3. The relaxation strength of the high-temperature process (α') constitutes about 10% of the total relaxation strength of the α and α' processes. The exact nature of these two different processes can only be speculated on. The different processes may occur in two different phases of ETP-rich material with different confinements.

The α process (main glass–rubber transition of the ETP-rich phase) occurs at significantly lower temperatures in the copolyesters than in the PETP homopolymer. Both dielectric measurements and DSC (Table I) reveal a T_g lowering of 20 °C in the 0.6–0.4 copolymer and of 10 °C in the 0.8–0.2 copolymer. These data are consistent with earlier data by Menczel and Wunderlich.[4] It should be noted that this lowering of the T_g occurs despite the introduction of the inflexible HBA units in the copolyesters. One possible explanation for this anomalous behavior is the existence of a plasticizing, oligomeric species in the ETP-rich component, although thermogravimetry (TG) of both copolyesters and of PETP did not indicate the presence of such material in the copolyesters.

The symmetric width parameter of the α process for the 0.6–0.4 copolymer is between 0.20 and 0.30, which is the same as has been reported[17] for semicrystalline PETP. The α process is too weak and too badly resolved in the 0.8–0.2 copolymer to constitute a sound basis for determination of the width parameter. Fully amorphous PETP exhibits a very narrow dielectric α transition with a width parameter between 0.8 and 0.9.[17] It is thus obvious that the α transition in the 0.6–0.4 copolymer is similar in this respect to the α process in semicrystalline PETP, which

indicates that the ETP-rich phase is to some extent constrained by the presence of the HBA-rich mesophase. The aforementioned lowering in temperature of the α transition of the copolymers with respect to that of PETP seems anomalous in view of the low value of symmetric width parameter observed for the 0.6–0.4 copolymer. However, at this stage no explanation can be given that fully reconciles these apparently contradictory findings.

Acknowledgment. The reported studies have been sponsored by the Swedish Natural Science Research Council (NFR), Grants K-RT 1910-100 and R-RA 1910-102, by the National Swedish Board for Technical Development (STU), Grant 85-5309, and by the National Science Foundation. The P(HBA–ETP) copolyesters and the PHBA homopolymer respectively were kindly supplied by Dr. Jackson, Eastman Co., TN, and Dr. Volksen, IBM Research, San Jose, CA.

Registry No. (Ethylene glycol)(*p*-hydroxybenzoic acid)(terephthalic acid) (copolymer), 25822-54-2.

References and Notes

(1) Roviello, A.; Sirigu, A. *J. Polym. Sci., Polym. Lett. Ed.* **1975**, *13*, 455.
(2) Jackson, W. J., Jr.; Kuhfuss, H. F. *J. Polym. Sci., Polym. Chem. Ed.* **1976**, *14*, 2043.
(3) Wooten, W. C.; McFarlane, F. E.; Gray, T. F., Jr.; Jackson, W. J., Jr. In *Ultra-High Modulus Polymers*; Ciferri, A., Ward, I. M., Eds.; Applied Science: London, 1979.
(4) Menczel, J.; Wunderlich, B. *J. Polym. Sci., Polym. Phys. Ed.* **1980**, *18*, 1433.
(5) Meesiri, W.; Menczel, J.; Gaur, U.; Wunderlich, B. *J. Polym. Sci., Polym. Phys. Ed.* **1982**, *20*, 719.
(6) Joseph, E. G.; Wilkes, G. L.; Baird, D. G. *Polym. Eng. Sci.* **1985**, *25*, 377.
(7) Joseph, E. G.; Wilkes, G. L.; Baird, D. G. *Polymer* **1985**, *26*, 689.
(8) Hedmark, P.; Jansson, J.-F.; Hult, A.; Lindberg, H.; Gedde, U. W. *J. Appl. Polym. Sci.*, in press.
(9) Zachariades, A. E.; Logan, J. A. *Polym. Eng. Sci.* **1983**, *23*, 797.
(10) Zachariades, A. E.; Navard, P.; Logan, J. A. *Mol. Cryst. Liq. Cryst.* **1984**, *110*, 93.
(11) Kresse, H.; Talrose, R. V. *Macromol. Chem., Rapid Commun.* **1981**, *2*, 369.
(12) Kresse, H.; Kostromin, S.; Shibaev, V. P. *Macromol. Chem., Rapid Commun.* **1982**, *3*, 509.
(13) Kresse, H.; Shibaev, V. P. *Macromol. Chem., Rapid Commun.* **1984**, *5*, 63.
(14) Zentel, R.; Strobl, G. R.; Ringsdorf, H. *Macromolecules* **1985**, *18*, 960.
(15) Blundell, D. J.; Buckingham, K. A. *Polymer* **1985**, *26*, 1623.
(16) Takase, Y.; Mitchell, G. R.; Odayima, A. *Polymer Commun.* **1986**, *27*, 76.
(17) Coburn, J.; Boyd, R. H. *Macromolecules* **1986**, *19*, 2238.
(18) Economy, J.; Volksen, W. In *The Strength and Stiffness of Polymers*; Zachariades, A. E., Porter, R. S., Eds.; Marcel Dekker: New York, 1983.

Macromolecular Stereochemistry: The Effect of Pendant Group Structure on the Axial Dimension of Polyisocyanates[1]

Mark M. Green,*[2a] Richard A. Gross,[2a] Charles Crosby III,[2b] and Frederic C. Schilling[2c]

Department of Chemistry and Polymer Research Institute, Polytechnic University, Brooklyn, New York 11201, Corporate Research and Development, Allied Corporation, Morristown, New Jersey 07960, and AT&T Bell Laboratories, Murray Hill, New Jersey 07974. *Received September 17, 1986*

ABSTRACT: The optically active and racemic forms of the 1,2 acetone ketal of propylene glycol were converted via the hydroxyl function to the derived isocyanates. These monomers were polymerized following Shashoua, using sodium cyanide in dimethylformamide at −65 °C. Light scattering determination in chloroform of the weight-average molecular weight and the root-mean-square radius of gyration ($\bar{M}_w$, $\langle S^2 \rangle^{1/2}$) shows, by estimates of the persistence lengths, that the optically active polymer (730 000, 1600 Å) has a more extended chain than its racemic derived isomer (500 000, 850 Å) and, based on the literature, is also more extended than poly(*n*-butyl isocyanate). The optically active polymer exhibited a circular dichroism spectrum ($\Delta\epsilon = -3$, $\lambda_{max} = 244$ nm) similar to that observed by Goodman and Chen on poly(2-methylbutyl isocyanate). The ultraviolet spectra showed an unusual sensitivity to the pendant group: the optically active and racemic derived polyisocyanates were similar ($\lambda_{max} = 238$ nm, $\epsilon = 2.4 \times 10^3$) and ($\lambda_{max} = 242$ nm, $\epsilon = 2.5 \times 10^3$) and differed from poly(*n*-butyl isocyanate) ($\lambda_{max} = 254$ nm, $\epsilon = 3.7 \times 10^3$). These data require the sense of the polyisocyanate helix to be related to the pendant group configuration and also demand the formation of a *d,l* copolymer in the polymerization of the racemic monomer. In addition, the results are consistent with helix reversals as important contributors to wormlike behavior in polyisocyanates. The 125.7-MHz carbon-13 NMR spectra showed broadened resonances for both backbone and side-chain nuclei in the isocyanate polymers as compared to random coil polymers. Further work is needed to separate the role of pendant group asymmetry and steric bulk in the conformational properties of the polyisocyanates.

Introduction

A variety of physical chemical probes demonstrate that poly(*n*-alkyl isocyanates) adopt wormlike conformations in solution.[3] In the solid state X-ray studies[4] show these polymers to exist in a helical conformation with eight monomer units in three turns and a pitch of 5.17 Å. This can be pictured as a cis–trans array with a 45° angle between the amide units.[3-6]

Although this helical characteristic is found to be consistent with the solution properties,[3,5,6] the dipole moment

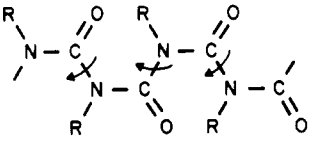

and the radius of gyration of the poly(*n*-alkyl isocyanates) are not prportional to the degree of polymerization, as expected for a rod, and the polymers are, therefore, best described as wormlike. Both the increasing number of

0024-9297/87/2220-0992$01.50/0